ANALYTICAL AND EXPERIMENTAL STUDY OF FRP-STRENGTHENED RC BEAM-COLUMN JOINTS

Dr. Costas P. Antonopoulos, University of Patras, Greece
Assoc. Prof. Thanasis C. Triantafillou, University of Patras, Greece

Abstract

Analytical models are presented in this study for the analysis of RC joints strengthened with composite materials. The models provide equations for stresses and strains at various stages of the response (before or after yielding of the beam or column reinforcement) until the ultimate capacity is reached, defined by concrete crushing or FRP failure due to fracture or debonding. Solutions to these equations are obtained numerically. The analytical formulation provides useful information on the shear capacity of FRP-strengthened joints in terms of the quantity and configuration of the externally bonded reinforcement and may be used to design FRP jackets for poorly detailed beam-column joints; an illustration is provided through a case study. Finally, the analytical model is compared with a series of test results and the agreement between theory and experiments is found satisfactory.

Introduction

To overcome the difficulties and some problems associated with traditional techniques for strengthening shear-critical RC joints, namely intensive labor, artful detailing, increased dimensions, corrosion protection and special attachments, recent research efforts have focused on the use of fiber reinforced polymers (FRP), that may be epoxy-bonded in the form of flexible sheets or strips, with fibers oriented properly so as to carry tension forces due to shear (see Figure 1a as a typical example).

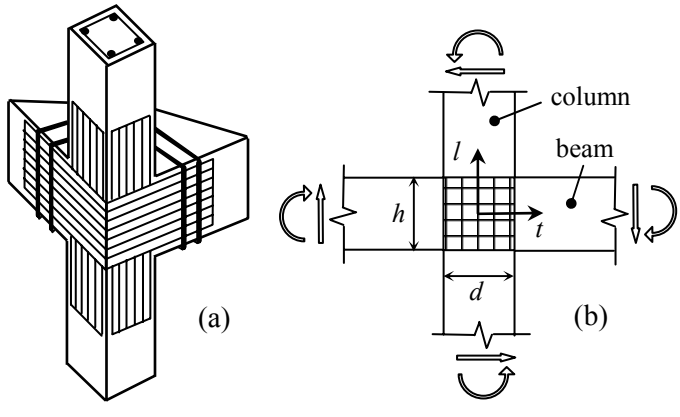

Figure 1. (a) Schematic illustration of RC joint strengthened with FRP (lines indicate direction of fibers). (b) Moment and shear acting at joint and definition of coordinate system.

Until now, FRP-strengthened joints have been studied mainly experimentally. Analytical modeling has been extremely limited and has led to oversimplified design approaches, failing to capture the real state of stress (and strain) in the joint.

On the other hand, analytical modeling of RC joints (without FRP) has been extensive. One of the most powerful models is that of Pantazopoulou and Bonacci (1992), which uses stress equilibrium and strain compatibility to yield the shear strength of a joint with known geometry and reinforcement quantities. In this study the authors have extended the aforementioned model to account for the effect of externally bonded FRP. They have also developed computer programs that may be used to trace the state of stress and strain in RC joints strengthened with either unidirectional strips or flexible sheets (the latter may be combined to form laminates). Following the analytical and numerical formulations one case study is analyzed and a comparison of the analytical model with existing test results is made.

Joints Strengthened with Sheets

Basic Assumptions

A typical beam-column joint is illustrated in Figure 1b. The joint is idealized as a three-dimensional element, with dimensions d (width of column), b (width of beam) and h (height of beam). Average stresses in the joint are shown in Figure 2a,b. Shear stresses are introduced by direct member action and by bond that develops between the main reinforcement and the joint core concrete. For simplicity, it is assumed that the shear stress, v, is uniformly distributed over the boundaries of the joint. Furthermore, it is assumed that at the moment of strengthening the joint is already loaded, so that a set of initial normal strains, ε_{ot} and ε_{ol} in the transverse (beam) and longitudinal (column) direction, respectively, and an initial shear strain, γ_o, have developed.

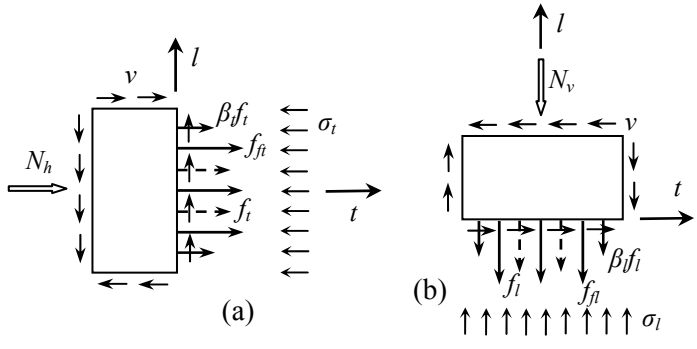

Figure 2. Stress equilibrium. (a) Horizontal forces; (b) vertical forces.

The principal strains, ε_1 and ε_2, are related to those in the longitudinal and transverse directions, ε_l, and ε_t, through the following expression:

$$tan^2\,\theta = \frac{\varepsilon_1 - \varepsilon_t}{\varepsilon_1 - \varepsilon_l} = \frac{\varepsilon_2 - \varepsilon_l}{\varepsilon_2 - \varepsilon_t} \tag{1}$$

where θ = inclination (from the t axis) of the maximum principal strain ε_1. Moreover, assuming that: (a) the maximum principal stress in the concrete, σ_1, cannot exceed the tensile capacity, which is taken zero; and (b) the directions of principal strains and stresses coincide (this is nearly correct if the reinforcement has not yielded), one may show that:

$$\sigma_t = -v\,tan\,\theta \tag{2}$$

$$\sigma_l = -\frac{v}{\tan\theta} \tag{3}$$

where σ_t and σ_l is the average compressive stress in the concrete in the transverse (t) and longitudinal (l) direction, respectively. Furthermore, with $\sigma_1 = 0$, the "stress invariant" condition gives the minimum principal stress in the concrete:

$$\sigma_2 = \sigma_t + \sigma_l \tag{4}$$

Finally, the shear strain γ in the joint equals:

$$\gamma = \frac{2(\varepsilon_1 - \varepsilon_t)}{\tan\theta} = \frac{-2\tan\theta(\varepsilon_l - \varepsilon_t)}{1 - \tan^2\theta} \tag{5}$$

Equilibrium Considerations

A key assumption in this section is that the FRP material consists of sheets or fabrics (with fibers in directions that do not coincide necessarily with the vertical and/or horizontal) that are stacked to form a laminate of thickness t_f. In this case the reinforcement ratio in each direction is $\rho_{ft} = \rho_{fl} = \rho_f = nt_f/b$, where n is the number of laminates ($n = 2$ for two-sided jackets, when both sides of the joint are accessible; $n = 1$ for one-sided jacket, when a transverse beam exists so that application of the jacket on both sides is not possible).

Stresses and strains in the composite material are coupled according to the following constitutive law:

$$\begin{bmatrix} f_{ft} \\ f_{fl} \\ f_{ftl} \end{bmatrix} = \begin{bmatrix} Q_{11} & Q_{12} & Q_{13} \\ Q_{12} & Q_{22} & Q_{23} \\ Q_{13} & Q_{23} & Q_{33} \end{bmatrix} \cdot \left(\begin{bmatrix} \varepsilon_t \\ \varepsilon_l \\ \gamma \end{bmatrix} - \begin{bmatrix} \varepsilon_{ot} \\ \varepsilon_{ol} \\ \gamma_o \end{bmatrix} \right) \tag{6}$$

where f_{ft} = average normal stress in the FRP in the transverse direction (at mid-width of the joint); f_{fl} = average normal stress in the FRP in the longitudinal direction (at mid-height of the joint); f_{ftl} = shear stress in the composite material; and Q_{ij} ($i, j = 1, 2, 3$) are elements of the composite material stiffness matrix that depend on the properties (four elastic constants and thickness) of the various laminae (layers) that have been stacked to form the joint's external reinforcement.

Horizontal force equilibrium requires that σ_t satisfy the following:

$$\sigma_t = -(\rho_s + \beta_t \rho_b) f_t - \rho_f [Q_{11}(\varepsilon_t - \varepsilon_{ot}) + Q_{12}(\varepsilon_l - \varepsilon_{ol}) + Q_{13}(\gamma - \gamma_o)] - \frac{N_h}{bh} \tag{7}$$

where f_t = average stress in the horizontal stirrups (at mid-width of the joint); ρ_s = stirrup reinforcement ratio; ρ_b = total main beam reinforcement ratio; β_t = factor with values between 0-1, relating the magnitude of stresses (or strains) in the main beam reinforcement to the average stirrup stresses (or strains) at the column centerline; and N_h = compressive axial force of the beam (if any). The factor β_t accounts for the bond conditions along the main beam reinforcement: for perfect bond, $\beta_t = 0$, for negligible bond $\beta_t = 1$ (Pantazopoulou and Bonacci 1992).

Similarly, vertical force equilibrium gives the average longitudinal compressive stress in the concrete, σ_l, as follows:

$$\sigma_l = -\left(\rho_{c,in} + \beta_l \rho_c\right) f_l - \rho_f \left[Q_{12}\left(\varepsilon_t - \varepsilon_{ot}\right) + Q_{22}\left(\varepsilon_l - \varepsilon_{ol}\right) + Q_{23}\left(\gamma - \gamma_o\right)\right] - \frac{N_v}{bd} \tag{8}$$

where f_l = average stress of longitudinal reinforcement of the column inside the joint core at the mid-height of the joint; $\rho_{c,in}$ = column reinforcement ratio inside the joint core; ρ_c = total main column reinforcement ratio (at the boundaries of the joint core); β_l = factor that relates the magnitude of stresses (or strains) in the main column reinforcement to the average stresses (or strains) of the reinforcement inside the core at the beam centerline; and N_v = compressive axial force of the column. As above, the factor β_l accounts for the bond conditions along the main column reinforcement (at the boundaries of the core).

To limit the number of variables in the problem, we make the following simplifications: $\rho_t = \rho_s + \beta_t \rho_b$ = effective horizontal reinforcement ratio, $\rho_l = \rho_{c,in} + \beta_l \rho_c$ = effective vertical reinforcement ratio. Moreover, we assume that the effective yield stress of the horizontal reinforcement, f_{yt}, is given as $f_{yt} = (\rho_s f_{sy} + \beta_t \rho_b f_{by})/\rho_t$, where f_{sy} = yield stress of stirrups and f_{by} = yield stress of beam reinforcement. The yield stress of the column reinforcement is denoted as f_{yl}. Next we analyze all the possible states of joint behavior.

Analysis before yielding of steel

We start with Equation 1 and the material constitutive laws:

$$tan^2\,\theta = \frac{\varepsilon_2 - \varepsilon_l}{\varepsilon_2 - \varepsilon_t} = \left(\frac{\sigma_2}{E_c} - \varepsilon_l\right)\left(\frac{\sigma_2}{E_c} - \varepsilon_t\right)^{-1} \tag{9}$$

where E_c = is the secant elastic modulus of concrete in the strain under consideration. The stress σ_2 is written in terms of v and tanθ using Equations 2-4. The resulting expression is:

$$-v n_{sc}\, tan^3\,\theta - \varepsilon_t E_s\, tan^2\,\theta + \frac{n_{sc} v}{tan\,\theta} + \varepsilon_l E_s \tag{10}$$

where $n_{sc} = E_s/E_c$. Next we write Equation 7 with σ_t replaced by $-v$tanθ, γ replaced by the right term in Equation 5 and $f_t = E_s \varepsilon_t$. The result is obtained in terms of v as follows:

$$v = \frac{1}{\tan\theta}\left[\rho_t E_s \varepsilon_t + \rho_f\left(Q_{11} + \frac{2Q_{13}\tan\theta}{1-\tan^2\theta}\right)\varepsilon_t + \rho_f\left(Q_{12} - \frac{2Q_{13}\tan\theta}{1-\tan^2\theta}\right)\varepsilon_l - \rho_f K_1 + \frac{N_h}{bh}\right] \tag{11}$$

where

$$K_1 = Q_{11}\varepsilon_{ot} + Q_{12}\varepsilon_{ol} + Q_{13}\gamma_o \tag{12}$$

Finally, we write Equation 6 with σ_l replaced by $-v/$tanθ, γ replaced by the right term in Equation 5, $f_l = E_s \varepsilon_l$ and v as given in Equation 9. The result in terms of ε_l is as follows:

$$\varepsilon_l = \frac{\left(\rho_t E_s + \rho_f A\right)\varepsilon_t - \rho_f\left(K_1 - K_2\tan^2\theta\right) + \frac{N_h}{bh} - \frac{N_v}{bd}\tan^2\theta}{\rho_f B + \rho_l E_s \tan^2\theta} \tag{13a}$$

where

$$A = \left(Q_{11} + \frac{2Q_{13}\tan\theta}{1-\tan^2\theta} \right) - \left(Q_{12} + \frac{2Q_{23}\tan\theta}{1-\tan^2\theta} \right) \tan^2\theta \tag{14}$$

$$B = -\left(Q_{12} - \frac{2Q_{13}\tan\theta}{1-\tan^2\theta} \right) + \left(Q_{22} - \frac{2Q_{23}\tan\theta}{1-\tan^2\theta} \right) \tan^2\theta \tag{15}$$

$$K_2 = Q_{12}\varepsilon_{ot} + Q_{22}\varepsilon_{ol} + Q_{23}\gamma_o \tag{16}$$

Analysis after yielding of effective horizontal reinforcement and before yielding of effective vertical reinforcement

The analysis is carried out as in 2.2.1 above with $f_t = f_{yt}$. Hence v is given by Equation 11 with the product $E_s\varepsilon_t$ replaced by f_{yt} and the expression for ε_l becomes:

$$\varepsilon_l = \frac{\rho_f A\varepsilon_t - \rho_f \left(K_1 - K_2 \tan^2\theta \right) + \frac{N_h}{bh} - \frac{N_v}{bd}\tan^2\theta + \rho_t f_{yt}}{\rho_f B + \rho_l E_s \tan^2\theta} \tag{13b}$$

Analysis after yielding of both horizontal and vertical reinforcement

The analysis is carried out as in 2.2.1 above with $f_t = f_{yt}$ and $f_l = f_{yl}$. Hence v is given by Equation 11 with the product $E_s\varepsilon_t$ replaced by f_{yt} and the expression for ε_l becomes:

$$\varepsilon_l = \frac{\rho_f A\varepsilon_t - \rho_f \left(K_1 - K_2 \tan^2\theta \right) + \frac{N_h}{bh} - \frac{N_v}{bd}\tan^2\theta + \rho_t f_{yt} - \rho_l f_{yl}\tan^2\theta}{\rho_f B} \tag{13c}$$

Analysis after yielding of effective vertical reinforcement and before yielding of effective horizontal reinforcement

Here too, the analysis is carried out as in 2.2.1 above with $f_l = f_{yl}$. The shear stress v is given by Equation 11 and ε_l is:

$$\varepsilon_l = \frac{\left(\rho_t E_s + \rho_f A \right)\varepsilon_t - \rho_f \left(K_1 - K_2 \tan^2\theta \right) + \frac{N_h}{bh} - \frac{N_v}{bd}\tan^2\theta - \rho_l f_{yl}\tan^2\theta}{\rho_f B} \tag{13d}$$

Compressive crushing of concrete

During any of the preceding states the concrete may crush; this will define failure of the joint. Crushing will occur when the principal compressive stress, σ_2, reaches the strength of concrete, f_c^{max}. The stress-strain relationship assumed here along the principal compressive direction is that described in Pantazopoulou and Bonacci (1992):

$$\sigma_2 = f_c^{\max}\left[2\frac{\varepsilon_2}{\varepsilon_{\max}} - \left(\frac{\varepsilon_2}{\varepsilon_{\max}} \right)^2 \right] \tag{17}$$

$$\text{where } \left\{ \begin{array}{l} f_c^{\max} = \lambda f_c \\ \varepsilon_{\max} = \lambda \varepsilon_o \\ \lambda = \dfrac{1 + \rho_{sv} \left| f_{ys} / f_c \right|}{0.8 - 0.34 \left(\varepsilon_1 / \varepsilon_o \right)} \end{array} \right\},$$

f_c and ε_o (= -0.002) are the compressive strength and failure strain of concrete in uniaxial compression (they both carry negative signs) and ρ_{sv} is the volume ratio of stirrups.

Failure of the FRP

The FRP will fail by tensile fracture when the tensile stress (f_{ft} or f_{fl}) reaches the tensile strength, f_{fu}. Debonding is treated here according to the fracture mechanics-based model of Holzenkämpfer (1994), as modified by Neubauer and Rostásy (1997). This model gives the maximum tensile stress in an FRP sheet of thickness t_f when debonding occurs, $f_{f,deb}$, in terms of the FRP elastic modulus parallel to the loading direction, E_f, the mean tensile strength of concrete, f_{ctm}, and the bond length, ℓ_b.

Solution procedure

The analytical formulation given above was implemented in a computer program that was specifically developed for the analysis of RC joints strengthened with FRP sheets. The user inputs a series of material and geometric characteristics and the program traces the state of stress and strain in the joint until failure. Input to the program consists of: (i) the geometric variables ρ_s, ρ_b, $\rho_{c,in}$, ρ_c, ρ_f; (ii) the bond condition variables β_t and β_l; (iii) the material properties f_c, f_{ctm}, ε_o for concrete and E_s, f_{yl}, f_{ys}, f_{yb} for steel; (iv) the geometric and elastic constants of the various laminae forming the FRP laminate (the program calculates automatically the elements Q_{ij} of the FRP stiffness matrix) and the failure criterion for fracture of the laminate; (v) the normalized axial forces N_v/bd and N_h/bh; and (vi) the initial strain ε_{ot} in the joint (at the moment of strengthening). Note that for the most common case of laminates with fibers in the two orthogonal directions (l and t), in (iv) above it is sufficient to define the ultimate FRP stress, $f_{fu,t}$ in the direction t and $f_{fu,l}$ in the direction l. Upper limits to the FRP stress are also introduced to account for debonding; these values are estimated as described in 2.2.6 using the approach described in the previous section with E_f taken equal to Q_{11} or Q_{22}, for the limiting values of f_{ft} or f_{fl}, respectively.

As a first step, the program calculates the initial strain ε_{ol} required to satisfy equilibrium of the joint (without the FRP). Next, the strain ε_t is incremented and through an iteration scheme Equations 10, 11 and 13 are solved for $\tan\theta$, v and ε_l. The value of ε_l is always obtained by solving the equation corresponding to the state that is active in each step. At the end of each step the program checks for FRP debonding or concrete crushing, which define the shear capacity v_{max} (at least equal to that of the joint as if no FRP had been applied, $v_{o,max}$).

In principle, E_c is to be obtained through a secant modulus iteration scheme at each step. However, extensive analyses performed by the authors on FRP-strengthened joints as well as by Pantazopoulou and Bonacci (1992) on RC joints without FRP led to the conclusion that quite similar results can be obtained without iteration by choosing E_c to be the secant modulus at peak stress; this value may be assumed equal to $2f_c/\varepsilon_o$, that is $E_c = 1000f_c$.

Numerical Study

In the preceding sections algebraic expressions were derived for stresses and strains in RC joints strengthened with FRP materials at various states of the steel reinforcement (elastic, post-yield). In this section the equations for joint shear strength are applied to a generic joint strengthened with flexible sheets applied in several layers (laminae). The joint is assumed reinforced with a lot more reinforcement in the column than in the beam (ρ_l = 0.015, ρ_t = 0.006). Each FRP layer (lamina) consists of unidirectional carbon fibers in an epoxy matrix and has the following elastic constants: elastic modulus parallel to the fibers $E_{\parallel}$ = 180 GPa, elastic modulus perpendicular to the fibers $E_{\perp}$ = 10 GPa, shear modulus $G_{\parallel,\perp}$ = 5 GPa and Poisson's ratio $\nu_{\parallel,\perp}$ = 0.25. For the concrete we assume f_c = 25 MPa and f_{ctm} = 1.97 MPa. For the yield strength of the steel reinforcement we take f_{yl} = 400 MPa and f_{yt} = 310 MPa. Finally N_h = 0 and ε_{ot} = 0.0002.

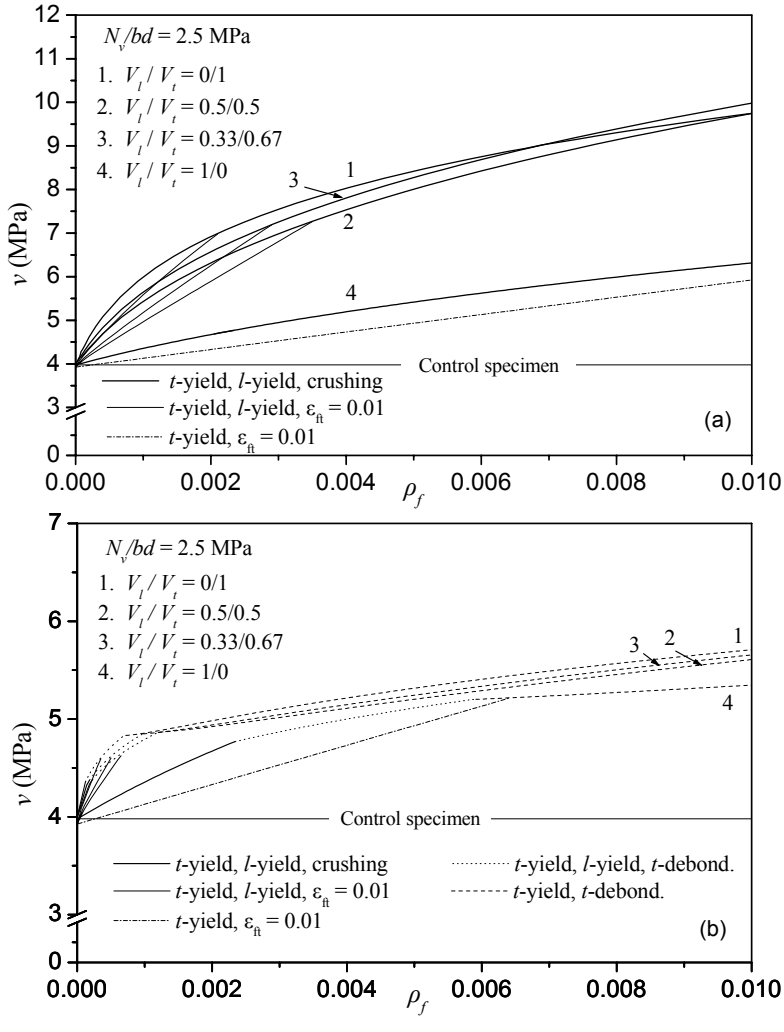

Figure 3. Shear strength of FRP-strengthened joint in terms of ρ_f for various fiber distributions. t-yield = yielding of beam reinforcement, l-yield = yielding of column reinforcement, t-debond. = debonding of beam reinforcement.

If FRP debonding is not a concern, absolute dimensions of the joint need not be specified, as they serve only to normalize steel/FRP quantities and axial loads. But if debonding dominates, we

need to know t_f, that is $b\rho_f/n$, and the FRP bond length in each direction. Hence, for each ρ_f we need to know the number of joint sides covered by the FRP (n = 1 or 2) and the width of the beam, b. In this case study b = 250 mm and n = 2. The bond lengths along the t and l directions are taken as ℓ_{bt} = 250 mm and ℓ_{bl} = 500 mm.

Next we define as V_l and V_t the volume fraction (within the laminate) of layers placed in the column and beam direction, respectively ($V_l + V_t = 1$). The following four configurations of the carbon sheets are assumed: (a) all layers with the fibers in the direction of the beam, V_l/V_t = 0/1; (b) the number of layers with fibers in the beam direction is the same as that in the column direction, V_l/V_t = 0.5/0.5; (c) the layers with fibers in the beam direction are two times more than those with fibers in the column direction, V_l/V_t = 0.33/0.67; and (d) all layers with the fibers in the direction of the column, V_l/V_t = 1/0. From the initial strain ε_{ot} before strengthening of the joints the other two elements of the initial strain matrix are calculated as follows: $\varepsilon_{ol} = -6.97\text{x}10^{-5}$ and $\gamma_o = 1.95\text{x}10^{-4}$.

Application of the procedure described above gives the shear strength of the joint in terms of the amount of FRP as shown in Figures 3a, b for N_v/bd = 2.5 MPa. Figure 3a applies if debonding is not of concern and Figure 3b applies with debonding taken into account. Each figure gives also the state of reinforcement at failure (steel may have yielded and the FRP may debond or fracture, at a hypothetical strain taken here equal to 0.01).

The general conclusion is that if debonding is not an issue, the effectiveness (increase in shear capacity, v) of FRP is quite substantial and, for a given ρ_f, it improves as more fibers are placed horizontally. This result is not surprising, as for this particular case study the joint steel reinforcement is much higher in the vertical direction than in the horizontal. If debonding is accounted for, the effectiveness of the FRP is relatively limited. Finally, FRP fracture is possible at low ρ_f only, and occurs in the horizontal (beam) direction.

Experimental verification

Experimental data on FRP-strengthened beam-column joints have been relatively limited. In order to validate the analytical model presented above and to obtain a more thorough understanding of the effect of various parameters on the behavior of RC joints, the authors conducted a comprehensive program that involved simulated seismic testing of approximately 2/3-scale T-joint models. The joints were poorly detailed (with no stirrups in the joint core) and the strengthening system was designed such that failure would occur due to shear. Earthquake loads were simulated by applying an alternating force (in a quasistatic cyclic pattern) to the end of the beam through an idealized pin and the axial force in the column was kept constant (Figure 4).

The displacement-controlled loading sequence for each specimen consisted of three cycles at a series of progressively increasing (by 5 mm) displacement amplitudes in each direction (push and pull), until a displacement of 45 mm was reached. Details about these tests may be found in the recent article of Antonopoulos and Triantafillou (2002). From the load versus displacement curves (see Figure 5 for some typical ones) it was possible to record the peak force, corresponding to joint failure, and based on that to calculate: (a) the tensile force T_b in the main beam reinforcement (calculated from cross section analysis); and (b) the shear force V_c at the column face. The quantity $(T_b - V_c)/bd$ gives the experimentally obtained value for the shear strength of the joint, v_{max}, which may be compared with the prediction of the analytical model.

Another set of similar - in principle - test results available in the literature is that of Gergely et al. (2000), who tested (differently detailed, compared to the above specimens) T-joints strengthened with CFRP and calculated the shear stress based on the experimentally measured load applied at failure of the joints.

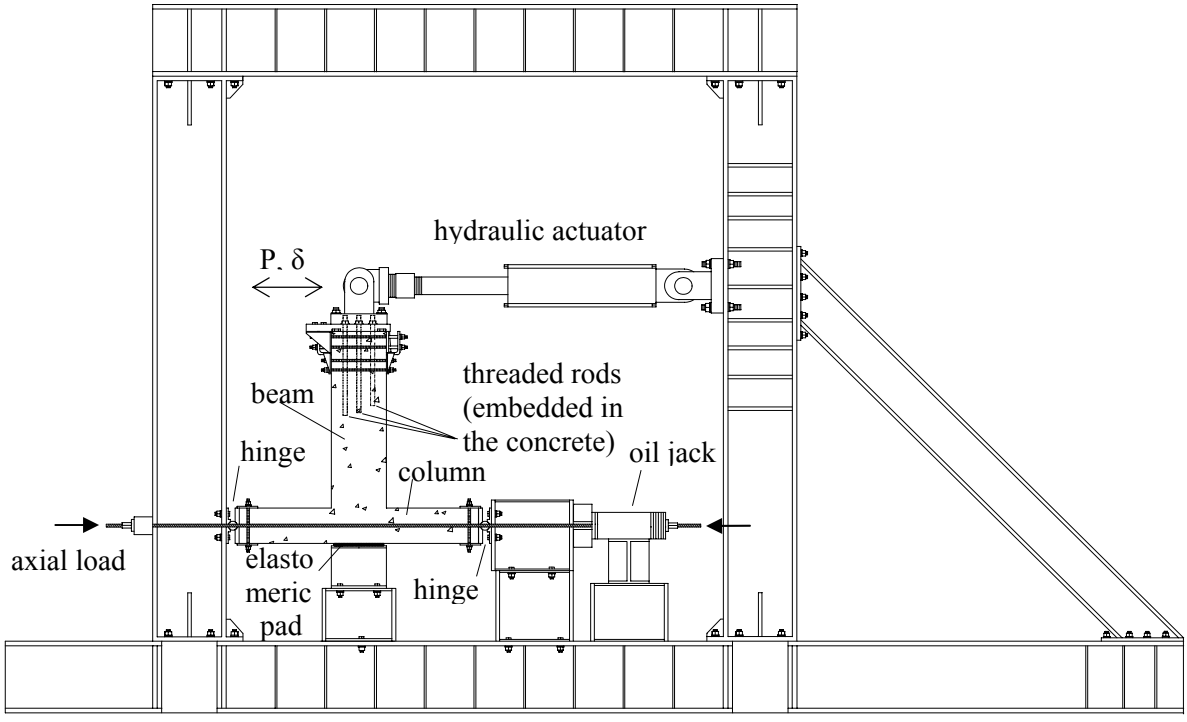

Figure 4. Schematic view of test setup and geometry of specimens.

Table 1. Design parameters of joints tested.

Specimen	f_c (MPa)	$\frac{N_v}{bd}$ (MPa)	(L/θ) [4]	t_f (mm)	ρ_f (x10^{-3})	E_{II} (GPa)
AT[1]						
F11	22.8	1.15	2/0°, 2/90°	0.13	2.6	230
F22	27.2	1.15	4/0°, 4/90°	0.13	5.2	230
F21	27.0	1.15	4/0°, 2/90°	0.13	3.9	230
F12	29.5	1.15	2/0°, 4/90°	0.13	3.9	230
F22W	29.2	1.15	4/0°, 4/90°	0.13	5.2	230
GL	19.5	1.15	5/0°, 5/90°	0.17	8.4	70
SF22[2]	19.0	1.15	4/0°, 4/90°	0.13	5.2	230
T-F33	26.0	1.15	3/0°, 3/90°	0.13	3.8	230
T-F22S2[3]	22.0	1.15	2/0°, 2/90°	0.13	2.6	230
GPR[1]						
4	20.0	0	2/45°, 2/-45°	1.32	15.0	64.7
8	20.0	0	2/45°, 2/-45°	1.32	15.0	64.7
9	20.0	0	2/45°, 2/-45°	1.32	15.0	64.7
12	34.0	0	2/45°, 2/-45°	1.32	15.0	64.7
13	34.0	0	2/45°, 2/-45°	1.32	15.0	64.7
14	34.0	0	2/45°, 2/-45°	1.32	15.0	64.7

[1] *AT*: Antonopoulos and Triantafillou (2002); *GPR*: Gergely et al. (2000). Notation of specimens is as defined by those who conducted the tests.
[2] $\rho_s = 0.0017$, $\rho_{sv} = 0.0034$, $f_y = 265$ MPa.
[3] Strips placed on one side of the joint debonded well before the peak load (strength) was reached and were ignored.
[4] L denotes the total number of layers on both sides of the joint at an angle θ from the horizontal.

Both sets of test data described above were used to evaluate the proposed analytical model. A few test results were omitted from the comparison, because the associated strengthening designs were considered as either unsuccessful or unrealistic: three joints in the study of Antonopoulos and Triantafillou (2002) were strengthened with stiff strips that debonded quite early (before the peak load was reached), whereas four joints in the study of Gergely et al. (2000) were strengthened with unrealistically low quantities (resulting in extremely low axial rigidity) of FRP. Details about the design parameters of the joints compared are given in Table 1 and the comparison between analytical and experimental values for the joint shear strength is given in Table 2. Unless described differently in Table 1, in all these tests ρ_s and $\rho_{c,in}$ were equal to zero and the bond of rebars was assumed perfect, corresponding to $\beta_t = \beta_l = 0$. The last assumption was verified in the tests of Antonopoulos and Triantafillou (2002), whereas no details are provided by Gergely et al. (2000) regarding rebar slip.

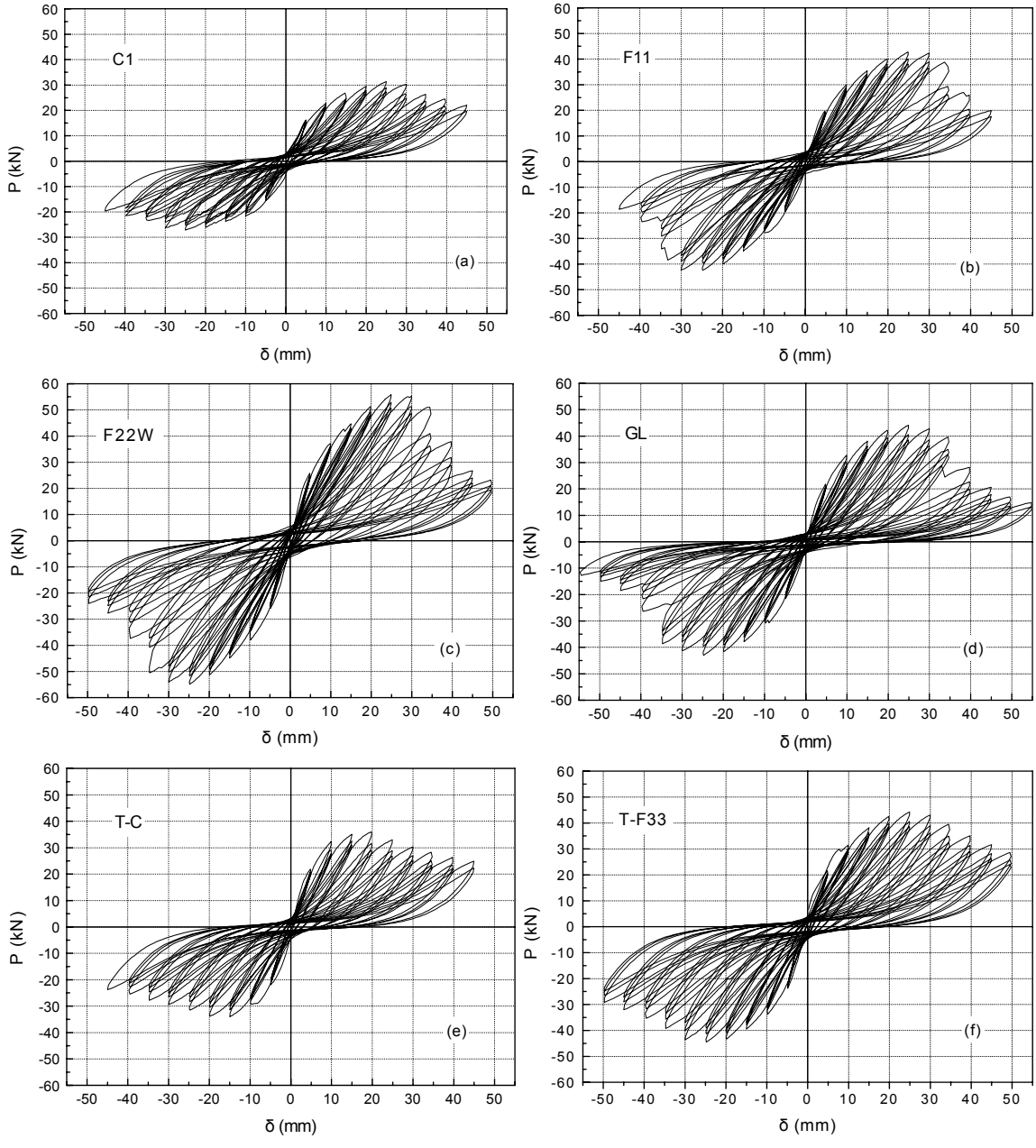

Figure 5. Typical load versus displacement curves.

Table 2. Comparison of analytical predictions with test results.

Specimen	v_{max} Experimental (MPa)	v_{max} Analytical (MPa)	$\frac{v_{max}\text{-Anal.}}{v_{max}\text{-Exp.}}$
AT			
F11	4.64	4.50	0.97
F22	5.37	6.62	1.23
F21	5.47	5.75	1.05
F12	4.74	5.84	1.23
F22W	6.15	6.88	1.12
GL	4.80	4.36	0.91
SF22	4.81	5.68	1.18
T-F33	4.80	5.66	1.18
T-F22S2	4.33	4.42	1.02
GPR			
4	2.36	3.04	1.29
8	2.36	3.04	1.29
9	2.56	3.04	1.19
12	2.59	3.04	1.17
13	2.58	3.04	1.18
14	2.96	3.04	1.02

The authors found the agreement between analysis and test results surprisingly good, and feel confident that the analytical procedure developed in this study may be used as a valuable tool towards the design of FRP jackets for shear strengthening of beam-column joints.

Conclusions

Analytical models are presented in this study for the analysis of RC joints strengthened with composite materials in the form of externally bonded jackets comprising strips or fabrics with fibers in any direction. The models provide equations for stresses and strains at various stages of the response until the ultimate capacity is reached, defined by concrete crushing or FRP failure due to fracture or debonding. Solutions to these equations are obtained numerically.

The models provide useful information on the shear capacity of FRP-strengthened joints in terms of the quantity and configuration of the externally bonded reinforcement and may be used to design FRP jackets for poorly detailed beam-column joints.

Parametric analyses indicate that even low quantities of FRP materials may provide significant enhancement of the shear capacity. The effectiveness of external reinforcement increases considerably if debonding is suppressed (e.g. through proper anchorage) and depends heavily on the distribution of layers in the beam and the column. The latter depends on the relative quantities of steel reinforcement crossing the joint panel and the level of axial load in the column.

Shear strength predictions provided by the analytical models were found in extremely good agreement with 15 experimental results found in the literature, thus adding confidence to the validity of the proposed equations.

Acknowledgements

Partial support to this research has been provided by the Research Committee of the University of Patras ("K. Karatheodoris" Program) and by the General Secretariat for Research and Technology (PENED 1999).

References

1. Antonopoulos, C.P. and Triantafillou, T.C. (2002), "Experimental Investigation of FRP-strengthened RC Beam-column Joints", *Journal of Composites for Construction*, ASCE, accepted.
2. Gergely, J., Pantelides, C.P. and Reaveley, L.D. (2000), "Shear strengthening of RC T-Joints using CFRP composites", *Journal of Composites for Construction*, ASCE, 4(2), pp. 56-64.
3. Holzenkämpfer, P., (1994), *Ingenieurmodelle des verbundes geklebter bewehrung für betonbauteile*, PhD dissertation, TU Braunschweig, Germany.
4. Neubauer, U. and Rostásy, F.S. (1997), "Design Aspects of Concrete Structures Strengthened with Externally Bonded CFRP-Plates", In *Concrete+Composites, Proceedings of the 7th International Conference on Structural Faults and Repair*, 2, pp. 109-118.
5. Pantazopoulou, S. and Bonacci, J. (1992), "Consideration of Questions about Beam-column Joints", *ACI Structural Journal*, 89(1), pp. 27-36.